

Scanning Electrochemical Microscopy in Neuroscience

Albert Schulte,¹ Michaela Nebel,²
and Wolfgang Schuhmann²

¹Biochemistry-Electrochemistry Research Unit, School of Chemistry and Biochemistry, Institute of Science, Suranaree University of Technology, Nakhon Ratchasima 30000, Thailand; email: schulte@sut.ac.th

²Analytische Chemie—Elektroanalytik und Sensorik, Ruhr-Universität Bochum, 44780 Bochum, Germany; email: wolfgang.schuhmann@rub.de

Annu. Rev. Anal. Chem. 2010. 3:299–318

First published online as a Review in Advance on
March 9, 2010

The *Annual Review of Analytical Chemistry* is online
at anchem.annualreviews.org

This article's doi:
10.1146/annurev.anchem.111808.073651

Copyright © 2010 by Annual Reviews.
All rights reserved

1936-1327/10/0719-0299\$20.00

Key Words

SECM, SICM, nervous system, secretion, neurotransmitter release, nanoelectrodes

Abstract

This article reviews recent work involving the application of scanning electrochemical microscopy (SECM) to the study of individual cultured living cells, with an emphasis on topographical and functional imaging of neuronal and secretory cells of the nervous and endocrine system. The basic principles of biological SECM and associated negative amperometric-feedback and generator/collector-mode SECM imaging are discussed, and successful use of the methodology for screening soft and fragile membranous objects is outlined. The drawbacks of the constant-height mode of probe movement and the benefits of the constant-distance mode of SECM operation are described. Finally, representative examples of constant-height and constant-distance mode SECM on a variety of live cells are highlighted to demonstrate the current status of single-cell SECM in general and of SECM in neuroscience in particular.

1. INTRODUCTION

A fundamental concern of neuroscience research is how the nervous system, which includes the brain, the spinal cord, and networks of sensory nerve cells (neurons), is structured so that it can be operationally coupled to its endocrine counterpart and other cellular entities for the orchestrated performance of the entire organism. Nervous system processes may be as fundamental as vision, smell, taste, hearing, breathing, digestion, balance, and movement, or they may be related to more complex mental processes such as behavior, consciousness, perception, learning, and memory. Furthermore, current neuroscience research also focuses on failures of the nervous system and their contribution to the onset of specific disease states such as dementia, Parkinson's disease, depression, addiction, memory loss, and schizophrenia. These investigations can lead to a knowledge-based development of effective medication for neuronal and mental disorders. Progress in all these areas relies on a complete understanding of the principles of neuronal activity on the molecular, cellular, systemic, and cognitive levels. As would be expected from the complexity of the subject and its interdisciplinary use among the fields of clinical, life, natural, and analytical sciences, numerous methodologies are used in a complementary fashion to determine the organization and functions of the nervous system and the principles of its multimode cell-to-cell messaging. In addition to general cellular and molecular biology techniques, investigators frequently employ modern genetic, immunological, and histochemical assays. These are used with model organisms and animal tests, bioinformatics, tailored analytical and electrophysiology detection schemes, and a wide range of modern microscopic imaging equipment. As shown in **Figure 1**, three major types of redox electrochemistry-related analytical assays are extensively used in experimental neuroscience. These assays include (*a*) *in vivo* voltammetry, (*b*) microdialysis in combination with an electrochemical manifestation of species in the perfusion solution (the dialysate), and (*c*) *in vitro* electroanalysis of the activity of isolated living target cells that may be cultured or available in (fresh) tissue slices.

In vivo voltammetry (1) started with the work of Adams and coworkers (2) almost 40 years ago. These authors, who sought to unravel the chemistry of neurotransmission and mental dysfunction, used minimally invasive current measurements at carefully implanted voltammetric microelectrodes as *in vivo* electrochemical probes, which made this technique a prominent detection scheme for monitoring in real time the dynamics of catecholamine neurotransmitters in the extracellular fluid of the brains of living laboratory rats kept under controlled conditions. Moderately invasive microdialysis (3, 4), an *in vivo* sampling method that is nearly as old as *in vivo* voltammetry, employs tiny catheter-type microdialysis tubes for the local collection of low-molecular-weight solutes released by the cells in the tissue where the device was implanted. By way of the semipermeable outer wall of the dialysis probe tip, the slowly flowing perfusion fluid is kept in continuous diffusional contact with the surrounding extracellular liquid matrix, and due to concentration gradients, targeted analyte species may diffuse into the tube interior. They are then transported by the stream of dialysate to a suitable detector. When microdialysis is used with voltammetric detection, the detector is a flow-through electrochemical cell.

For *in vitro* electroanalysis of individual nerve and endocrine cells, the tips of needle-type voltammetric microelectrodes are placed in close proximity to the plasma membrane of the target cell with a micropositioning device mounted on an inverted microscope. After positioning the tip, one can record changes in the chemical composition of the cell surroundings—possibly induced by secretory and/or metabolic cell processes—in real time by operating the sensor in one of several voltammetric modes, provided that the compounds released or consumed through cellular events are intrinsically redox active. The success of such a single-cell electroanalytical approach is demonstrated by progress in, for instance, our understanding of (*a*) the mechanism of

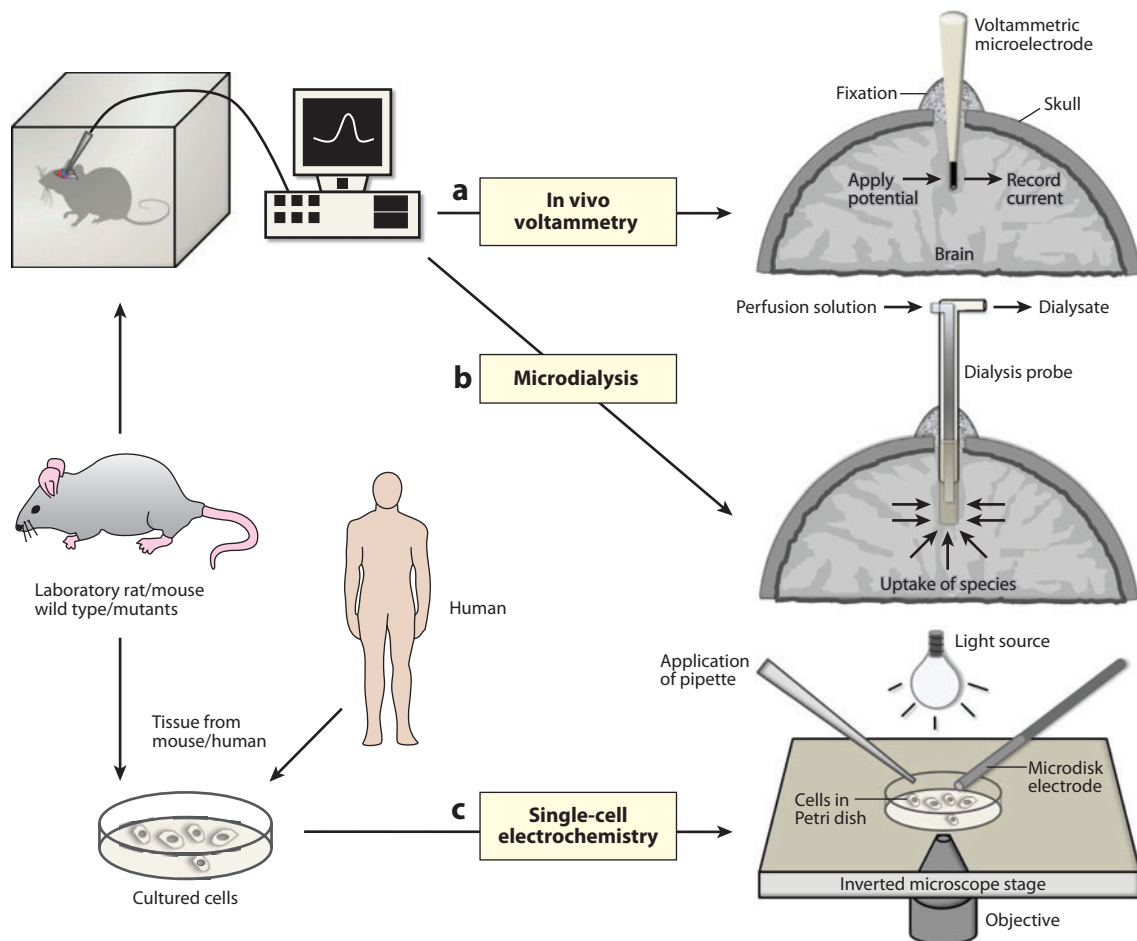


Figure 1

Redox electrochemistry-based analytical assays used in neuroscience. (a) In vivo voltammetry performed with brain-implanted carbon or noble-metal microelectrodes. Neurotransmitters or other chemical species in the extracellular brain fluid are identified and quantified through both their oxidation or reduction at the properly polarized electrode surface and the analysis of associated current flow. (b) In vivo microdialysis. Catheter-type implanted microdialysis probes collect analytes from the region of the semipermeable membranes via diffusional interaction with the brain fluid. The perfusate is brought to an electrochemical flow-through cell and subjected to electroanalysis. (c) Single-cell electrochemistry. Individual cultured cells are selected with an inverted microscope and are approached with the tiny tips of disk-shaped microelectrodes. Upon stimulation with suitable agents, changes in the cell environment are traced with, for instance, (fast) cyclic voltammetry or amperometry.

Ca^{2+} -dependent vesicular release of chemical messengers from secretory cells and isolated neurons and (b) the phenomenon of oxidative cell stress (5–11).

A strength of in vivo voltammetry and microdialysis is that they draw information from the intact regulatory cell network of a living, alert animal with ongoing physiological and mental activity, which is obligatory for pharmacokinetic and cognitive behavioral studies. Monitoring neurochemical changes in response to actions as, for example, food and drug self-administration was approached by what was recently defined as psychoanalytical electrochemistry (12). However, electrochemical studies in the controllable, scaled-down setting of cultured model cells are better

for resolving the general molecular mechanisms behind intercellular signal communication, as well as nerve and endocrine cell metabolism, respiration, growth, and apoptosis. Evaluating chemical processes in a physiological buffer solution in a culture dish is simpler than evaluating them in the highly heterogeneous *in vivo* matrix, which contains many other cells and various chemical substances unrelated to the process being evaluated. Scanning electrochemical microscopy (SECM) for spatially resolved measurements on cultured cells was a natural and important extension of conventional single-cell voltammetry.

Cellular SECM also employs tiny, precisely positioned disk-shaped microelectrodes—SECM tips—for analyte detection. In cellular SECM experiments, however, the tip is not kept stationary after being brought close to the cell but rather is scanned over the object so that it can determine the cell topography along with a complete two-dimensional image of a particular cellular function. In Section 2, we provide details about the instrumental design and operational principles of SECM and describe some promising applications of single-cell SECM. In Section 3, we describe the specific technical prerequisites for SECM experiments on living cells and discuss the state of the art in terms of the equipment and strategies used in advanced single-cell SECM. We refer the reader to a number of excellent reviews and book chapters (5–11, 13–21) that address single-cell electroanalysis, cellular SECM, and SECM in neuroscience as complementary sources of information. In Section 4, we evaluate recent literature on the closely related technique of scanning ion conductance microscopy (SICM), which employs tiny ionic currents through a scanned micropipette tip (22) rather than faradaic currents from redox reactions at a disk electrode for object analysis. SICM has been applied to cultured cell studies to reveal cell (membrane) topography and the location and opening times of membrane-integrated ion channels.

2. CELLULAR SCANNING ELECTROCHEMICAL MICROSCOPY

2.1. Principles and Relevant Technical Details

SECM (23) is a noncontact electrochemical variant of scanning probe microscopy first suggested in the 1980s by Engstrom et al. (24) and Bard et al. (25). SECM was initially used to study interfacial processes in physical chemistry and materials science (20, 21, 23, 26–30); however, its potential as a tool for examining biological samples was soon realized. Biological applications other than studies of cultured cells, which are the focus of this article, include studies of the local activity of immobilized enzyme microstructures (31, 32), the flux of species through protein channels in lipid bilayer membranes (33–35) or pores in skin (36), fingerprint imaging (37) and the oxygen permeability of cartilage (38), label-free readout of hybridization at DNA chips (39), protein electrophoresis gels (40), and the probing of phase-transfer dynamics at dental interfaces *in vitro* (41, 42).

In addition to the standard components of electrochemical workstations—namely the amplifier (potentiostat), the reference electrodes and counterelectrodes, the electrochemical cell containing an electrolyte solution, and the operational software used to execute the planned experiments—SECM uses microelectrodes that are attached to a precise x,y,z -positioning device. This device permits the SECM tip to be scanned, allowing controlled voltammetry in space. To support the identification of healthy cells and to allow prealignment of the tip relative to a selected cell, one should install the SECM apparatus for cell measurements atop an inverted microscope containing a video system suitable for coarse-cell and electrode-tip visualization. For noninvasive SECM data/image acquisition on cells resting on a coverslip in a culture dish, the SECM tip is scanned in a horizontal plane at a chosen tip-to-sample separation (d , the working distance) at which the current through the polarized microelectrode develops as a function of the topographic profile

and/or the identity of the sample beneath the tip. Scanning at predefined secure height prevents the sample from being touched by the tip.

In a generic operation, SECM of single cultured cells employs a combination of the negative-feedback mode and the substrate (i.e., cell) consumption–tip collection (TC; also known as detection) mode of SECM for topography and physiological cell activity imaging, respectively. In TC mode, a properly polarized SECM probe is placed close to the cell membrane, where it functions as a voltammetric sensor with the ability to oxidize or reduce chemical species that are either released or consumed by the cell under observation. If topography effects are excluded, variations in the tip current reproduce changes in the flux of the species; these changes are thus a measure of the local cellular activity in terms of secretion or uptake.

To run the negative-feedback mode of SECM for cell-topography imaging, a hydrophilic, nonhazardous, and reversible redox compound must be added to the electrolyte solution and utilized as an electron-transfer mediator. The SECM tip detects the presence of the redox mediator, and a constant current is recorded as long as the tip is kept in bulk solution at a constant potential that is high enough to invoke the electrode reaction at a diffusion-limited rate. Both biological cells, containing hydrophobic lipid bilayer membranes, and glass slides are insulators and act as a barrier for hydrophilic mediator molecules. Proximity of the SECM tip to the coverslip of the cell leads to a decrease in the tip current, as compared with the bulk value, due to blocked diffusional mass transport of the redox species to the tip surface; this effect is referred to as negative feedback. When SECM is carefully performed, both approach curves (i.e., observations of the tip current as a function of gradually decreasing vertical tip position) over the glass slide at the side of a cell and an estimate of the dimension of the studied cells are used to position the tip exactly as high as needed to keep the tip from crashing into the cell during scanning. The SECM tip is then horizontally moved, and variations in the tip current or in the reading of the *z*-positioning unit are recorded in the constant-height and constant-current modes, respectively. The current variations in the SECM images obtained in negative-feedback mode reflect cell morphology and shape. Knowledge of the cell's topography is useful in determining the alignment between the tip and the cell for subsequent measurements of cell activity in TC mode.

Of special concern for cellular SECM applications is the design of the scanned microelectrode tip. SECM tips are usually disk-shaped electrodes made of Au and Pt microwires or carbon fibers and have diameters of a few micrometers (43). The ratio between the radius of the insulating sheath and the radius of the electroactive disk is known as the RG factor, which for nonbiological SECM measurements should be on the order of ten to gain an optimum blockade of mediator diffusion toward the encapsulated electrode and thus the best possible negative feedback. However, smaller RG values are indispensable for cellular SECM, given that single living cells are microscopic objects and SECM tips with a bulky insulation at the apex are difficult to position close to the cell membrane in a nondestructive way. Conical beveling of glass-insulated SECM tips or the use of miniaturized Pt, Au, or carbon electrodes insulated with thin layers of polymer films is necessary for the positioning and imaging of single cells in SECM.

2.2. Selected Applications of Cellular Scanning Electrochemical Microscopy in Feedback/Constant-Height Mode

Numerous SECM studies have been performed on single living cells in the above-described feedback/constant-height mode of SECM, demonstrating SECM's ability to image cellular processes. The feedback current establishes the cell location. This information is then used to place the tip at, for instance, the center of the object prior to taking activity measurements in TC mode. The references given in this section are not complete but rather reflect the wide range of

opportunities the method offers. Cell functions such as respiration or photosynthesis have been visualized with this procedure (44–46), as have the effects of heavy metal-induced stress on plant cells (47) and the antibacterial (48) and cytotoxic (49) effects of dissolved species on bacterial and other cells. Through use of hydrophobic and hence membrane-permeable (rather than hydrophilic and membrane-impermeable) redox mediators, a SECM-based detection scheme for intracellular redox activity was established and used to differentiate between healthy and cancerous cells (50). Dual-electrode SECM tips with bare and porphyrin-modified Pt disks were positioned at precise distances from endothelial cells and used to accurately acquire nitric oxide (NO) profiles in membrane-near zones (51). Furthermore, amperometric microbiosensors (rather than bare microdisk electrodes) were used as SECM tips to reveal (*a*) local hydrogen peroxide levels in the environment of a cell (52), (*b*) ATP transport through porous polycarbonate membranes under physiologically relevant conditions (53), and (*c*) profiles of glucose uptake above a single living cell (54).

More recently, conventional SECM cell studies addressed the imaging and detection of morphological changes of endothelial cells in response to stimulated NO release (55), the quantification of cytosolic enzyme activity (56), the recognition of epidermal growth factor receptors at cell membranes (57), the screening of protein solubility in bacterial cells (58), the enhancement of cellular Ag^+ uptake via cell exposure to an inhibitor of voltage-sensitive K^+ ion channels (59), the realization of a predictive method to perform a quality assessment of pancreatic islets on the basis of SECM measurements of glucose-stimulated respiratory activity (60), the detection of oxygen and hydrogen peroxide variations during an oxidative burst of macrophages (61), and the investigation of the interaction between live cells/their membranes and metal nanoparticles (62). Finally, the topography of PC12 cells (which are dopamine-releasing model cells used for the study of neuronal function), the nerve growth factor-induced development of PC12 cell neurites, and the reversible changes in PC12 cell height in response to exposure to hypo- and hypertonic electrolyte solutions were assessed with reasonable resolution in the negative-feedback/constant-height mode of SECM (63).

The alternating-current response of a SECM tip to a sinusoidal excitation voltage, particularly in a low-conductance and mediator-free electrolyte solution, depends on the tip-to-sample separation and the nature of the approached interface. Knowledge of this relationship allowed investigators to develop alternating-current SECM (AC-SECM) (64), which has been used in numerous materials science applications to visualize interfacial variations of local electrochemical activity (65). More recently, AC-SECM on isolated African green monkey kidney cells showed that the alternating current-feedback response of the SECM tip scanned at fixed height in mediator-free electrolyte solution can also be used for visualizing cell morphologies, which may provide a useful alternative to imaging in amperometric-feedback mode, certainly in cases in which the presence of a mediator would inflict stress on the cells under investigation (66).

2.3. Scanning Electrochemical Microscopy Cell Imaging in Amperometric-Feedback/Constant-Height Mode: Limitations and Solutions

The most striking attribute of SECM used for living cell studies is undoubtedly its ability to reveal, in a more direct, nonlabeling, and dynamic fashion than any other (probe) microscopy technique, both the cellular landscape and valuable information about chemical identity and reactivity in the cell's environment. The spatial resolution that can be achieved depends mostly on the dimension of the electrode disk, which forms the sensing component of the SECM tip; thus, investigators are pursuing a reduction in electrode size to the nanometer scale. As depicted in **Figure 2**, nanoelectrode-based SECM is crucial for the realization of true neuroscience SECM.

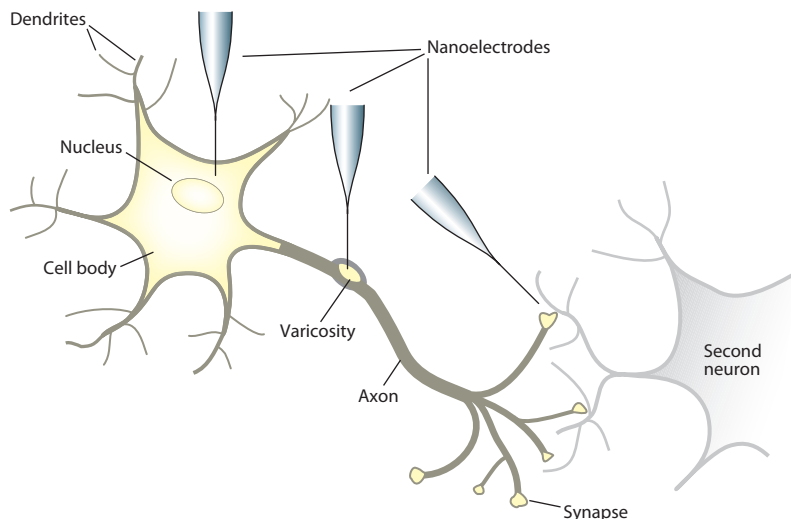


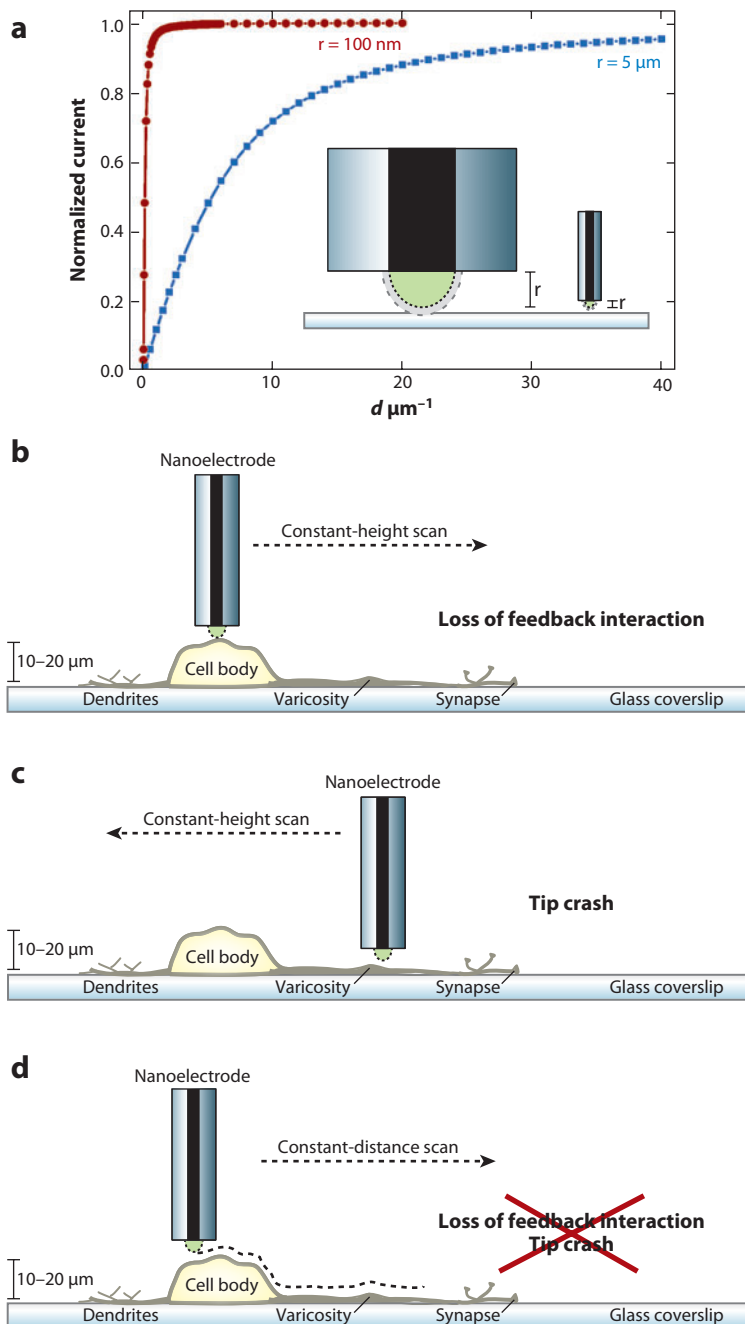
Figure 2

Neuroscience scanning electrochemical microscopy (SECM) simultaneously provides topographic and local functional information about networks of neuronal cells. Topographical information is a prerequisite for the exact positioning of the SECM tip at predefined areas of the cell body, at a varicosity, or above a synapse. Following tip placement, voltammetry is used to take high-spatial-resolution local measurements of secretory or metabolic activity.

The goal is to perform high-resolution topographical and electrochemical analysis of (*a*) (networks of) neurons whose branching communicative axons and dendrites are much smaller than the micrometer-sized neuronal cell bodies themselves and (*b*) submicrometer-sized varicosities that arise from the projections for nonsynaptic neurotransmitter release.

Voltammetric nanosensors that are suitable for very high resolution cellular imaging have previously been described (67–81). However, inspection of normalized SECM approach curves for micro- and nanoelectrodes shows that use of nanoelectrode SECM tips to image three-dimensional cellular structures is problematic in conventional negative-feedback/constant-height mode. **Figure 3a** displays theoretical negative-feedback *z*-approach curves that were calculated for 5- μm -radius and 100-nm-radius disk electrodes following existing modeling (82). The two approach curves suggest that a suitable value for *d* is equal to or less than the diameter of the SECM tip. For imaging purposes, submicrometer-scale electrodes should therefore be scanned at a submicrometer distance from the obstructing surface or object; this requirement poses a challenge for the imaging of neuronal features whose heights are very dissimilar. If a nanoelectrode SECM tip is positioned in proper feedback distance above the center of a neuron, and if a scan in the horizontal direction is later initiated at fixed height, loss of feedback appears as soon as the tip moves away from its position above the cell body (**Figure 3b**). However, the tip can crash into the cell, causing neuron damage, if the nanoelectrode feedback positioning is done, for instance, above an axon, a varicosity, or a dendrite (**Figure 3c**). Therefore, the constant-height mode of tip movement should be replaced by the constant-distance mode, in which the tip closely follows the contours of a cell structure in a nondestructive manner (**Figure 3d**). Automated distance control for SECM tips has been realized through a computer-controlled feedback loop, which reacts to distance variations between the probe and the sample by immediately repositioning the tip in the vertical direction and returning to the user-defined set point for the tip-to-sample separation.

Suitable distance-dependent input signals for such an integrated SECM distance-control unit are the vibration amplitude of an oscillating SECM tip as measured with optical (83–86), piezo-electric (87), and tuning fork–based (78, 88–91) schemes; the amperometric SECM tip current (89, 92–94); or the SECM tip impedance (93, 95–97). The use of atomic force microscopy (AFM) with cantilever-integrated microelectrodes provides another means of achieving constant-distance



electrochemical and topographical imaging (98–101). Whether implemented into a SECM device or an AFM device, a constant-distance scan not only avoids tip crash and loss of feedback contact but also provides topographic information.

SECM has been combined not only with AFM but also with scanning near-field optical microscopy (SNOM) (78, 89, 102, 103). The advantage of using tapered optical glass fibers with integrated ring micro- or nanoelectrodes in a hybrid SECM/SNOM system is that fluorescent cell (membrane) labeling can be employed as an extra tool to mark and identify specific sections on cell structures. In principle, this allows the SECM tip to approach spots on cell surfaces that are distinguished from their surroundings by specific fluorescence.

3. APPLICATIONS OF CONSTANT-DISTANCE MODE SCANNING ELECTROCHEMICAL MICROSCOPY TO STUDIES OF CELLULAR PROCESSES

If not carried out as a SECM-AFM experiment, high-resolution cellular SECM in constant-distance mode requires (a) one of the above-described distance-control modes for accurate tip positioning and (b) a low-noise electrochemical workstation for sensitive current measurement via micro- or nanoelectrodes. Near-field optical analysis may also be integrated if SNOM functionality is desired. Visual inspection of cells and the SECM tip requires that the SECM components are placed atop the stage of an inverted microscope. Good vibration dampening is necessary for trouble-free data acquisition. Several laboratories have recently established cellular constant-distance electrochemical microscopy, either as biological SECM (BIO-SECM; see **Figure 4**) or integrated in an AFM setup; however, few studies have been published on constant-distance mode topography and SECM imaging of living cells, regardless of their type.

A BIO-SECM instrument that uses shear force-based distance control and 1–5- μm -diameter carbon fiber microdisk electrodes as amperometric SECM tips was applied for sequential topography and local chemical transmitter release measurements at individual chromaffin cells that were obtained from the medulla of a bovine adrenal gland (86). Success with the recordings of vesicular exocytosis on both types of sensors confirmed the functionality of constant-distance SECM on cells that are widely used as a model system for unraveling the mechanism of chemical cell-to-cell communication. Nerve growth factor-induced PC12 cell differentiation into neuron phenotypes was visualized through use of a BIO-SECM instrument that took advantage of constant current- or impedance-based distance regulation and carbon ring or carbon fiber SECM

Figure 3

Constant-height mode versus constant-distance mode of scanning electrochemical microscopy (SECM). (a) Theoretical approach curves displaying the negative amperometric-feedback effect that occurs when a microdisk or nanodisk electrode with a radius of 5 μm or 100 nm is brought toward an insulating surface. The gray semicircle below the disk represents the hemispherical diffusion field of the miniaturized electrodes. I (current) was calculated (according to Reference 82) assuming an RG (radius of insulating sheath/radius of enclosed conductive disk) value of 10. At a negative-feedback current of approximately 70% of the diffusion-limited value in infinite distance, the working distance is equal to the active tip diameter. Thus, the smaller the tip is, the closer it has to be to the surface during scanning to be in feedback contact. (b) Negative-feedback contact, as established right above a living cell, is lost during scanning in constant-height mode. (c) Tip crash into a cell takes place if the SECM tip is positioned in proximity to, for instance, a dendrite, then scanned at constant height toward the cell body. (d) Overcoming the limitations of constant-height mode SECM as depicted in panels b and c by means of the constant-distance mode. Readings of the z-positioning device, which responds to local changes in the contours of the scanned object, provide information about cell topography.

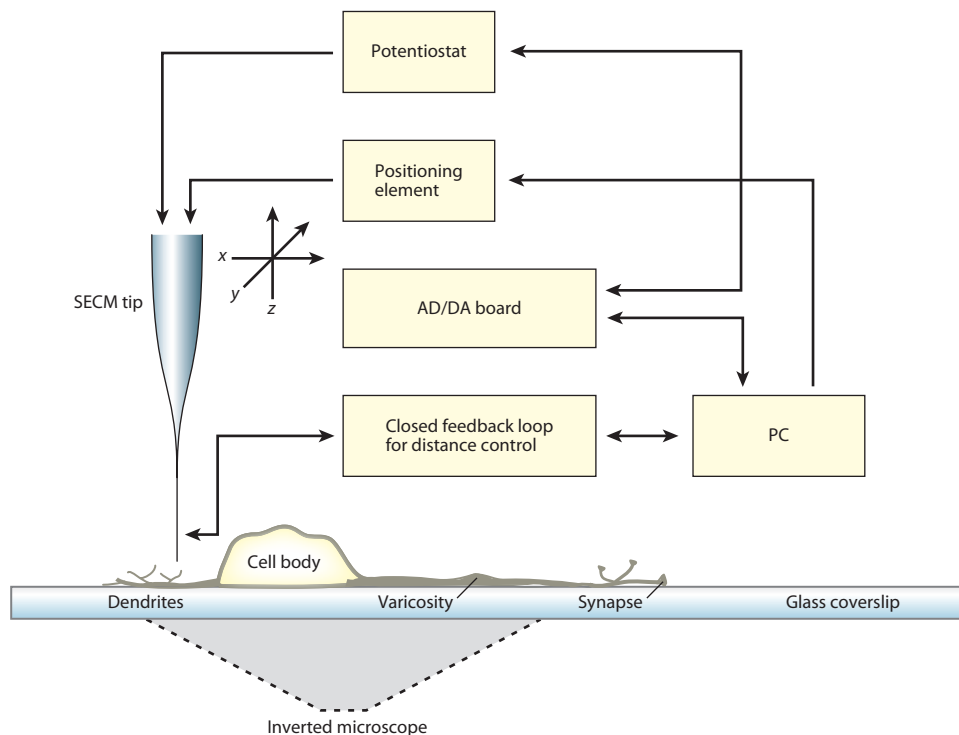


Figure 4

A biological scanning electrochemical microscopy (BIO-SECM) device for high-resolution topographical and chemical imaging of single living cells in constant-distance mode. The main components of the customized SECM are the micropositioning system for supporting precise SECM tip movements, an inverted optical microscope for visualizing the SECM tip and the cells, a low-noise electrochemical amplifier, an analog-to-digital and digital-to-analog converter (AD/DA board) for data acquisition and potential application, a feedback-loop distance control for maintaining a defined tip-to-surface separation, and a personal computer (PC) for system control.

tips (93). SECM topography images of both emerging neurites and older, longer neurites with bifurcations and beaded varicosities were made. Moreover, the system allowed amperometric detection of vesicular catecholamine release after positioning the tip at places of interest. Notably, the shear force- and impedance-based distance-control modes, unlike their constant-current analog, operate in pure cell growth media without redox mediator addition, which is an asset for long-term investigations of events such as neuronal network development and/or degeneration. Hybrid SECM/SNOM (102) and SECM/SNOM/AFM (103) microscopes with specially designed bi- or trifunctional tips were used in two other studies to image differentiating PC12 cells. Again, both embryonic and mature neurites as well as varicosity-like structures were observed, but in this case the topographic images were acquired via dynamic-force AFM and the optical images were taken via SNOM detection of fluorescent-labeled cytosolic Ca^{2+} ions. The topographic information gained from AFM and SNOM scans performed immediately prior to SECM was used to guide the probe tip over preidentified features to acquire electrochemical images in negative-feedback mode.

Combined topographical, optical, and electrochemical images of living cells and cell activity taken via the standing approach (STA) mode of SECM (91) were used to partly overcome

inherent problems of the extremely close positioning distance in shear force mode (78). The STA methodology involves a shear force/tuning fork–based positioning of vibratable SECM tips, such as needle-type glass capillaries, optical fibers, glass capillary electrodes, and optical fiber electrodes, for topographical, optical, joint topographic/electrochemical, and combined topographic/optical/electrochemical imaging, respectively. The dampening of the tip vibration, as detected by the tuning fork, is used during z approach to bring the tip at a given x,y coordinate of the imaging grid into gentle contact with the cell. The SECM tip is then retracted by 0.1 to 3 μm via the z -positioning device. At this well-defined tip-to-cell separation, electrochemical and/or optical data acquisition is performed. Plots of the vertical tip positioning, as well as the optical and electrochemical tip response as a function of the x,y coordinate, provide the SECM images. STA-SECM performed with tapered glass capillary tips is sufficiently sensitive to resolve the topography of single differentiated PC12 cells to the level of the axons and cell bodies under physiological conditions. When the tip consists of an electrode that is polarized to a potential sufficient for O_2 reduction, STA-SECM not only allows visualization of the axon and cell body topography but simultaneously reveals their individual contributions to cell respiration (**Figure 5**). Additionally, images of fluorescently dye-stained, differentiated PC12 cells can be obtained with optical fiber tips operated in STA-SECM mode.

Needle-type NO sensors were prepared based upon carbon fiber microelectrodes that were modified with an NO-selective Pt/Ni-phthalocyanine coating. These NO sensors were used as tips in a shear force–dependent, constant-distance SECM, and they can accurately trace the contours of single transformed human umbilical vein endothelial cells (104). Line scans allow a reproducible, nonmanual positioning of an NO sensor adjacent to the transformed human umbilical vein endothelial cell membrane at a distance of 100 to 300 nm. With the microsensor in such close proximity, stimulated NO release can be detected because most of the liberated NO is collected and electrochemically oxidized before it can escape through the narrow gap between the cell and tip.

4. CELLULAR SCANNING ION CONDUCTANCE MICROSCOPY

SICM (22) is a noncontact, high-resolution surface-imaging technique that is particularly suitable for living-cell contour profiling and cellular membrane topography measurements (105, 106). The SICM tip is an electrolyte-filled tapered glass nanopipette containing an Ag/AgCl electrode inserted into it from the top. A bias potential between the inner electrode and another Ag/AgCl electrode, which is located in the bath solution, drives an ionic current flow through the pipette opening, which provides a distance-dependent signal. Thus, topographic information can be obtained because, at decreasing distances between the SICM tip and an object, the ion pathway becomes obstructed, leading to a concomitant decrease in the measured ion current. Initially, a direct-current ionic current was used to derive SICM images; however, for nondestructive, highest-resolution SICM imaging of soft samples, specific distance-control modes for the acquisition of local current/surface profiles may be preferable. Examples are the shear force method (107, 108), as is also used with SECM and SNOM; the alternating-current mode with a vibrating nanopipette (109); and the pulse mode (110) and closely related hopping mode (111) of SICM. In both the pulse mode and the hopping mode, SICM has been employed for imaging living cells and their membranes under physiological conditions. **Figure 6** displays a representative SICM image of a cultured astrocyte from postnatal rat hippocampus acquired via floating backstep mode. With this approach, short current pulses of small amplitude are applied to the SICM tip, and the voltage for current generation is measured. Values distant to the sample surface define the basal resistance, R . The SICM pipette is then brought toward the sample

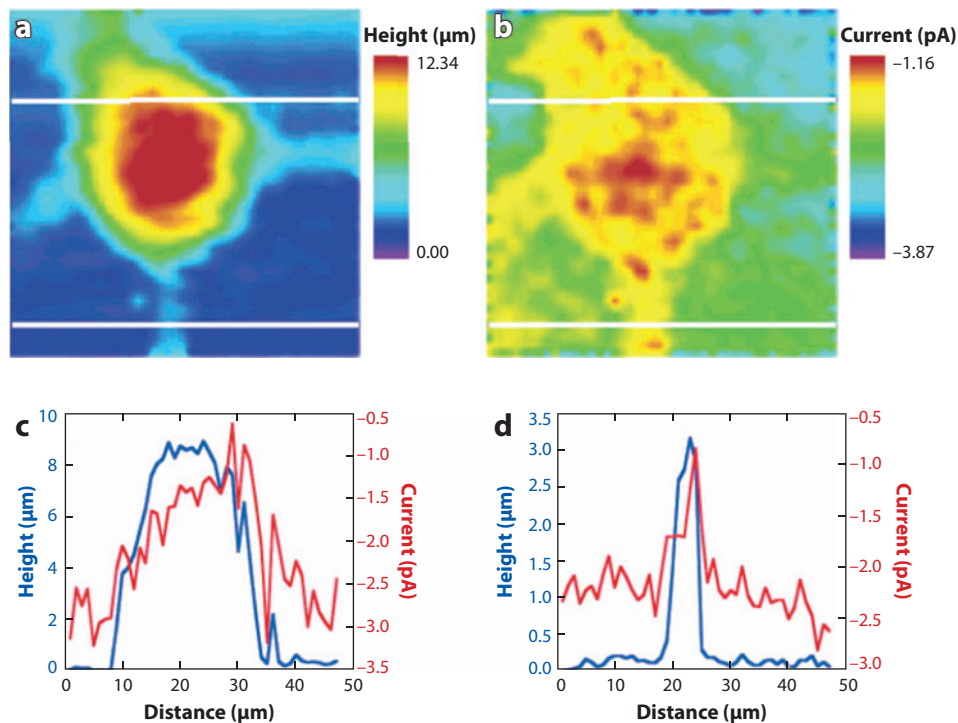


Figure 5

(a) Topography and (b) scanning electrochemical microscopy (SECM) images of a differentiated PC12 cell in a physiological buffer solution. The images, with a scan range of $47\ \mu\text{m} \times 47\ \mu\text{m}$, were obtained in the standing approach (STA) mode of SECM via a capillary electrode probe. Panel a is based on the shear force signal arising from the hydrodynamic interaction of the needle-type glass capillary with the surface; this panel represents the topography of the cell. Panel b reflects the oxygen profile at a given separation between the SECM tip and the cell membrane. The electrode of the scanned probe was held at a potential sufficient to reduce oxygen ($-0.5\ \text{V}$ versus Ag/AgCl). (c) Topographical information and (d) the electrochemical measure of oxygen consumption from the cross sections (white lines in panels a and b) at the cell body and at an axon, respectively. Reproduced from Reference 78 with permission.

until R passes an upper limit. The x , y , and z coordinates at the position of the R threshold are stored and used to form the sample topography from sequentially measured grid points with equal R changes. For fast, nondestructive cell-topography imaging, a low-resolution prescan is performed, and the information obtained is then used to guide the probe securely over the cell in subsequent high-resolution scans (112). Cellular SICM was used to study the dynamics of cell volumes (112–114), membrane-near Ca^{2+} levels together with contours of contracting cardiac myocytes (115), proteins in the plasma membrane (116), embryonic stem cell–derived cardiomyocytes (117), morphological parameters of somata and neurites of cultured neurons (118), changes in cell membrane morphology associated with exocytosis (119), and functional localization of single active ion channels on living-cell membranes (120). Moreover, SICM is suitable for guiding and redirecting neuronal growth cones of the leech (121) as well as for carrying out localized and noncontact mechanical stimulation of human dorsal root ganglion sensory neurons (122).

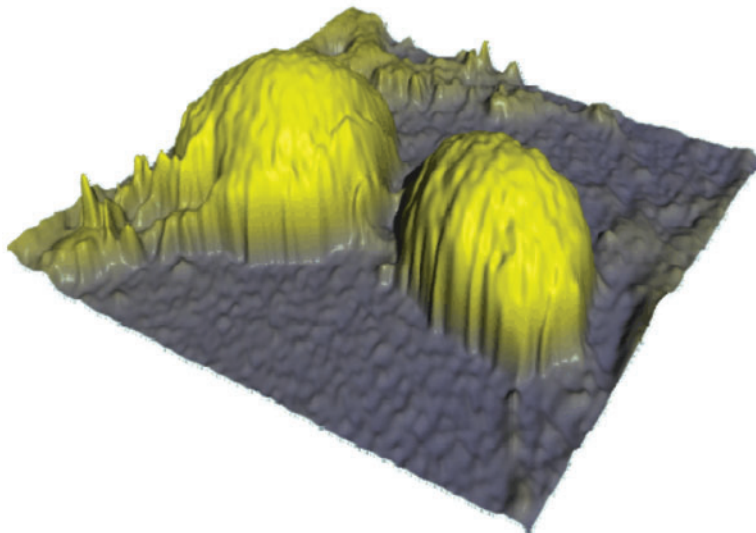


Figure 6

Images of two oligodendrocytes from adult pig brain acquired via scanning ion conductance microscopy in floating backstep mode. Scanning was performed with a glass electrode ($\sim 1\ \mu\text{m}$ opening diameter) filled with an extracellular bath electrolyte solution containing 145 mM NaCl, 4 mM KCl, 3 mM CaCl_2 , 2 mM MgCl_2 , 10 mM glucose, and 10 mM HEPES. The bath solution has a pH of 7.2, and the resistance through the pipette tip is approximately 5 M Ω . The scan area is $50 \times 50\ \mu\text{m}^2$, the lateral step size is $1\ \mu\text{m}$, and the horizontal step size is 100 nm. Reproduced courtesy of P. Happel and I.D. Dietzel, Ruhr-Universität Bochum.

5. CONCLUSION AND FUTURE PROSPECTS

Just over 20 years ago, SECM emerged as a fascinating electrochemical surface-imaging technique, and soon thereafter, the first successful inspections of the topography and activity of living cells were performed. The following decade saw significant technical and procedural improvements in the methodology and optimization of SECM hardware and software features. Additionally, the development of novel schemes for SECM tip fabrication and positioning, as well as signal utilization, allowed the performance of micro- and nanoscale SECM experiments (in both materials and life sciences) that otherwise would not have been possible. As for neuroscience applications, modern SECM with micro- and nanoelectrodes proved capable of high-spatial-resolution imaging of the structural and functional details of individual neuronal and endocrine cells. However, to progress from the single-cell level to true prognostic neuroscience, as well as to gain information about (a) communicating networks of multiple cells, (b) cellular cross talk, and (c) developmental, degenerative, and pharmacological modulations of neurotransmission and cell morphology, further advances in SECM techniques will be needed. SECM imaging of sample areas containing more than one cell is only possible if improved scanning and sampling modes are implemented and if SECM tips that can secure more stable topographical and electrochemical responses are available. To address this issue, our laboratory is testing a four-dimensional, shear force–based constant-distance mode for SECM (4D-SFCD-SECM). As with the above-mentioned STA mode (78, 91), acquisition of a single data point at a predefined x,y grid point of the SECM image arises from (a) a noncontact tip approach into the shear force interaction region (approximately 100 nm above the surface), (b) retraction of the tip for a defined increment, (c) storage of the

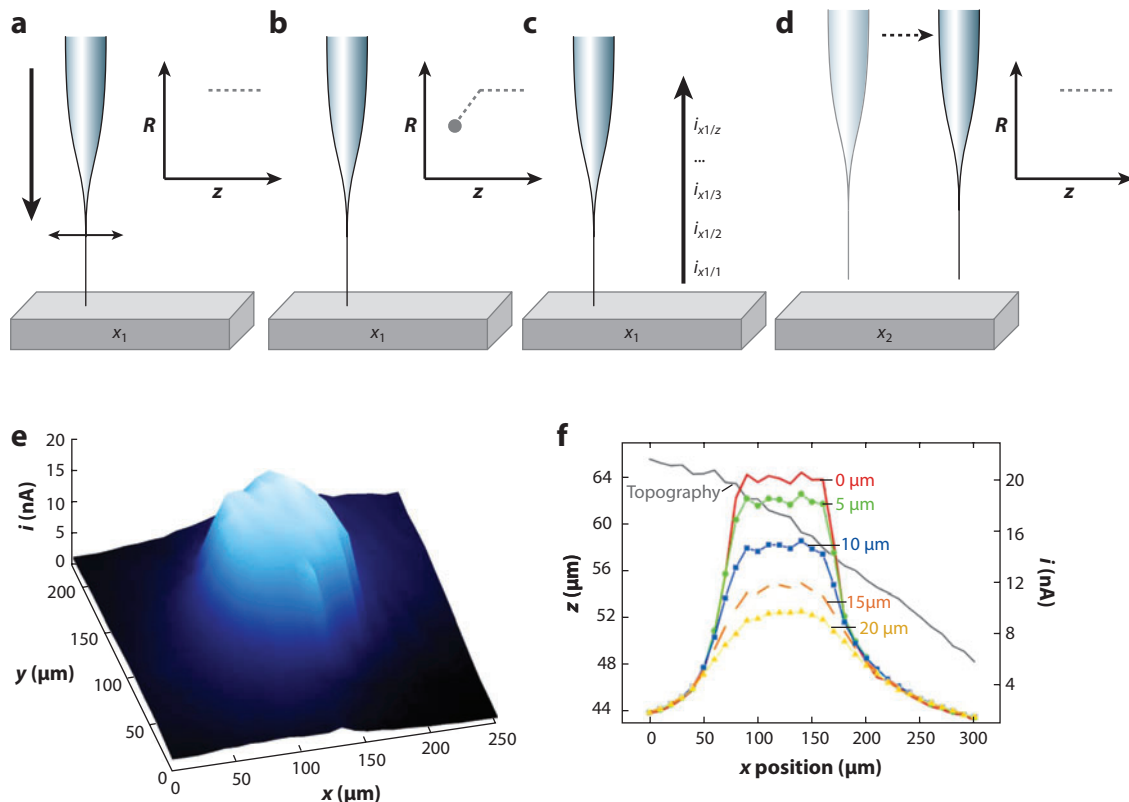


Figure 7

(a–d) Principle of the four-dimensional, shear force-based constant-distance mode for scanning electrochemical microscopy (4D-SFCD-SECM mode) and (e,f) visualization of the diffusion field of electrochemically generated $[\text{Ru}(\text{NH}_3)_6]^{2+}$ in 4D-SFCD-SECM with a generator-/collector-type arrangement. (a) The electrode is vibrated at resonance frequency and approached under shear force control to the sample surface. (b) The approach halts when a user-defined stop point (i.e., a certain change in vibration amplitude) is reached. (c) This point corresponds to the point of closest approach and represents the sample topography. The z -piezo position and the corresponding current signal are stored before the electrode is retracted in predefined increments with simultaneous current detection. Thereafter, the electrode is moved to the next grid point (d), and the procedure is repeated. The current at the smallest tip-to-sample distance (defined as 0 μm) is plotted against the x,y position (e) and in different tip-to-sample separations as x -line scans (f). The electrode vibration frequency is 347 Hz. The shear force-based approach of the carbon fiber electrode (diameter of $\sim 8 \mu\text{m}$) was stopped at a change of 5% of the lock-in signal. The sample is a 100- μm Pt disk electrode in 100 mM KCl containing 5 mM $[\text{Ru}(\text{NH}_3)_6]^{3+}$. Abbreviation: R , magnitude of the lock-in detected shear force signal that reflects the tip vibration amplitude.

associated electrochemical response and reading of the displacement of the z -positioning element, and (d) plots of the values obtained as a function of their horizontal coordinates. The fourth dimension in a 4D-SFCD-SECM image—namely height-dependent current information—is then established by retracting the tip to a second (and third, and so on) tip-to-sample separation and recording the electrochemical information at each distance from the topography approach point detected during shear force approach. **Figure 7** shows a proof of principle of the proposed 4D-SFCD-SECM mode.

Currently, a thorough parameter optimization of 4D-SFCD-SECM for cellular applications is in progress. Although the technique is too slow to capture, for instance, fast vesicular transmitter release, its potential for studies of slower processes such as drug or toxin-induced changes in cell

morphology, metabolism, and health state, is considerable. Overall, SECM studies of neurons and endocrine cells have good prospects and are expected to further contribute to our understanding of the regulatory nervous and endocrine systems, single neurons, and secretory cells.

DISCLOSURE STATEMENT

The authors are not aware of any affiliations, memberships, funding, or financial holdings that might be perceived as affecting the objectivity of this review.

LITERATURE CITED

1. Robinson DL, Hermans A, Seipel AT, Wightman RM. 2008. Monitoring rapid chemical communication in the brain. *Chem. Rev.* 108:2554–84
2. Kissinger PT, Hart JB, Adams RN. 1973. Voltammetry in brain tissue—a new neurophysiological measurement. *Brain Res.* 55:209–13
3. Lunte CE, Scott DO, Kissinger PT. 1991. Sampling living systems using microdialysis probes. *Anal. Chem.* 63:773–78A
4. Watson CJ, Venton BJ, Kennedy RT. 2006. In vivo measurements of neurotransmitters by microdialysis sampling. *Anal. Chem.* 78:1391–99
5. Travis ER, Wightman RM. 1998. Spatio-temporal resolution of exocytosis from individual cells. *Annu. Rev. Biophys. Biomol. Struct.* 27:77–103
6. Jackson MB, Chapman ER. 2006. Fusion pores and fusion machinery in Ca^{2+} -triggered exocytosis. *Annu. Rev. Biophys. Biomol. Struct.* 35:135–60
7. Neher E. 2006. A comparison between exocytotic control mechanisms in adrenal chromaffin cells and a glutamatergic synapse. *Pflüg. Arch.* 453:261–68
8. Schulte A, Schuhmann W. 2007. Single-cell microelectrochemistry. *Angew. Chem. Int. Ed.* 46:8760–77
9. Adams KL, Puchades M, Ewing AG. 2008. In vitro electrochemistry of biological systems. *Annu. Rev. Anal. Chem.* 1:329–55
10. Amatore C, Arbault S, Guille M, Lemaitre. 2008. Electrochemical monitoring of single cell secretion: vesicular exocytosis and oxidative stress. *Chem. Rev.* 108:2585–621
11. Wang W, Zhang SH, Li LM, Wang ZL, Cheng JK, Huang WH. 2009. Monitoring of vesicular exocytosis from single cells using micrometer and nanometer-sized electrochemical sensors. *Anal. Bioanal. Chem.* 394:17–32
12. Venton BJ, Wightman RM. 2003. Psychoanalytical electrochemistry: dopamine and behavior. *Anal. Chem.* 75:414–21A
13. Yasukawa T, Kaya T, Matsue T. 2000. Characterization and imaging of single cells with scanning electrochemical microscopy. *Electroanalysis* 12:653–59
14. Brehm-Stecher BF, Johnson EA. 2004. Single-cell microbiology: tools, technologies, and applications. *Microbiol. Mol. Biol. Rev.* 68:538–59
15. Schulte A, Schuhmann W. 2006. Scanning electrochemical microscopy as a tool in neuroscience. In *Frontiers in Neuroengineering Series*, Vol. 1: *Electrochemical Methods for Neuroscience*, ed. AC Michael, LM Borland, pp. 353–72. Boca Raton: Taylor & Francis
16. Bard AJ, Li X, Zhan W. 2006. Chemically imaging living cells by scanning electrochemical microscopy. *Biosens. Bioelectron.* 22:461–72
17. Edwards MA, Martin S, Whitworth AL, Macpherson JV, Unwin PR. 2006. Scanning electrochemical microscopy: principles and applications to biophysical systems. *Physiol. Meas.* 27:R63–108
18. Ameniya S, Guo JD, Xiong H, Gross DA. 2006. Biological applications of scanning electrochemical microscopy: chemical imaging of single living cells and beyond. *Anal. Bioanal. Chem.* 386:458–71
19. Roberts WS, Lonsdale DJ, Griffiths J, Higson SPJ. 2007. Advances in the application of electrochemical microscopy to bioanalytical systems. *Biosens. Bioelectron.* 23:301–18
20. Sun P, Laforge FO, Mirkin MV. 2007. Scanning electrochemical microscopy in the 21st century. *Phys. Chem. Chem. Phys.* 9:802–23

21. Amemiya S, Bard AJ, Fan FRF, Mirkin MV, Unwin PR. 2008. Scanning electrochemical microscopy. *Annu. Rev. Anal. Chem.* 1:95–131
22. Hansma PK, Drake B, Marti O, Gould SA, Prater CB. 1989. The scanning ion-conductance microscope. *Science* 243:641–43
23. Bard AJ, Mirkin MV, eds. 2001. *Scanning Electrochemical Microscopy*. New York: Marcel Dekker
24. Engstrom RC, Weber M, Wunder DJ, Burgess R, Winquist S. 1986. Measurements within the diffusion layer using a microelectrode probe. *Anal. Chem.* 58:844–48
25. Bard AJ, Fan FRF, Kwak J, Lev O. 1989. Scanning electrochemical microscopy. Introduction and principles. *Anal. Chem.* 61:132–38
26. Bard AJ, Fan FRF, Pierce DT, Unwin PR, Wipf DO, Zhou F. 1991. Chemical imaging of surfaces with the scanning electrochemical microscope. *Science* 254:68–74
27. Bastos AC, Simoes AM, Gonzalez S, Gonzalez-Garcia Y, Souto RM. 2005. Applications of the scanning electrochemical microscope to the examination of organic coatings on metallic substrates. *Prog. Org. Coat.* 53:177–82
28. Lu X, Wang Q, Liu X. 2007. Recent applications of scanning electrochemical microscopy to the study of charge transfer kinetics. *Anal. Chim. Acta* 601:10–25
29. Wittstock G, Burchardt M, Pust SE, Shen Y, Zhao C. 2007. Scanning electrochemical microscopy for direct imaging of reaction rates. *Angew. Chem. Int. Ed.* 46:1584–617
30. Szunerits S, Pust SE, Wittstock G. 2007. Multidimensional electrochemical imaging in material science. *Anal. Bioanal. Chem.* 389:1103–20
31. Wittstock G. 2001. Modification and characterization of artificially patterned enzymatically active surface by scanning electrochemical microscopy. *Fresenius J. Anal. Chem.* 370:303–15
32. Stoica L, Neugebauer S, Schuhmann W. 2008. Scanning electrochemical microscopy (SECM) as a tool in biosensor research. *Adv. Biochem. Eng. Biotechnol.* 109:455–92
33. Guo J, Amemiya S. 2005. Permeability of the nuclear envelope at isolated *Xenopus* oocyte nuclei studied by scanning electrochemical microscopy. *Anal. Chem.* 77:2147–56
34. Wilburn JP, Wright DW, Cliffl DE. 2006. Imaging of voltage-gated alamethicin pores in a reconstituted bilayer lipid membrane via scanning electrochemical microscopy. *Analyst* 131:311–16
35. Jackson TJ, Sanderson JM, Katakly R. 2008. A gramicidin analogue that exhibits redox potential-dependent cation influx. *Sens. Actuators B* 130:630–37
36. Scott ER, White HS, Bradley Phipps J. 1993. Ionophoretic transport through porous membranes using scanning electrochemical microscopy: application to in vitro studies of ion fluxes through skin. *Anal. Chem.* 65:1537–45
37. Zhang M, Girault HH. 2009. SECM for imaging and detection of latent fingerprints. *Analyst* 134:25–30
38. Gonsalves M, Barker AL, Macpherson JV, Unwin PR, O'Hare D, Winlove CP. 2000. Scanning electrochemical microscopy as a local probe of oxygen permeability in cartilage. *Biophys. J.* 78:1578–88
39. Turcu F, Schulte A, Hartwich G, Schuhmann W. 2004. Label-free electrochemical recognition of DNA hybridization by means of modulation of the feedback current in SECM. *Angew. Chem. Int. Ed.* 43:3482–85
40. Zhang M, Wittstock G, Shao Y, Girault HH. 2007. Scanning electrochemical microscopy as a readout tool for protein electrophoresis. *Anal. Chem.* 79:4833–39
41. Nagues S, Denault G. 1996. Scanning electrochemical microscopy: amperometric probing of diffusional ion fluxes through porous membranes and human dentine. *J. Electroanal. Chem.* 408:125–49
42. Unwin PR, Macpherson JV, Beeston MA, Evans NJ, Littlewood D, Hughes NP. 1997. New electrochemical techniques for probing transfer dynamics at dental interfaces in vitro. *Adv. Dent. Res.* 11:548–59
43. Fan FRF, Demaille C. 2001. The preparation of tips for scanning electrochemical microscopy. In *Scanning Electrochemical Microscopy*, ed. AJ Bard, MV Mirkin, pp. 75–144. New York: Marcel Dekker
44. Yasukawa T, Kaya T, Matsue T. 1999. Dual imaging of topography and photosynthetic activity of a single protoplast by scanning electrochemical microscopy. *Anal. Chem.* 75:4637–41
45. Tsionsky M, Cardon ZG, Bard AJ, Jackson RB. 1997. Photosynthetic electron transport in single guard cells as measured by scanning electrochemical microscopy. *Plant Physiol.* 113:895–901
46. Takii Y, Takoh K, Nishizawa M, Matsue T. 2003. Characterization of local respiratory activity of PC12 neuronal cell by scanning electrochemical microscopy. *Electrochim. Acta* 48:3381–85

47. Zhu R, Macfie SM, Ding Z. 2005. Cadmium-induced plant stress investigated by scanning electrochemical microscopy. *J. Exp. Bot.* 56:2831–38
48. Holt KB, Bard AJ. 2005. Interaction of silver(I) ions with the respiratory chain of *Escherichia coli*: an electrochemical and scanning electrochemical microscopy study of the antimicrobial mechanism of micromolar Ag^+ . *Biochemistry* 44:1321–23
49. Mauzeroll J, Bard AJ, Owhadian O, Monks TJ. 2004. Menadione metabolism to thiodione in hepatoblastoma by scanning electrochemical microscopy. *Proc. Natl. Acad. Sci. USA* 101:17582–87
50. Rosenberg SA, Mirkin MV. 2004. Scanning electrochemical microscopy: detection of human breast cancer cells by redox environment. *J. Mammary Gland Biol. Neoplasia* 9:375–82
51. Isik S, Etienne M, Oni J, Blöchl A, Reiter S, Schuhmann W. 2004. Dual microelectrodes for distance control and nitric oxide release from endothelial cells by means of scanning electrochemical microscopy. *Anal. Chem.* 76:6389–94
52. Horrocks BR, Schmidke D, Heller A, Bard AJ. 1993. Scanning electrochemical microscopy. 24. Enzyme ultramicroelectrodes for the measurement of hydrogen peroxide at surfaces. *Anal. Chem.* 65:3605–14
53. Kueng A, Kranz C, Mizaikoff B. 2005. Imaging of ATP membrane transport with dual microdisk electrodes and scanning electrochemical microscopy. *Biosens. Bioelectron.* 21:346–53
54. Ciobanu M, Taylor DE, Wilburn JP, Cliffel DE. 2008. Glucose and lactate biosensors for scanning electrochemical microscopy imaging of single live cells. *Anal. Chem.* 80:2717–27
55. Wang W, Xiong Y, Du FY, Huang WH, Wu WZ, et al. 2008. Imaging and detection of morphological changes of single cells before and after secretion using scanning electrochemical microscopy. *Analyst* 132:515–18
56. Gao N, Wang X, Li L, Zhang X, Jin W. 2007. Scanning electrochemical microscopy coupled with intracellular standard addition method for quantification of enzyme activity in single intact cells. *Analyst* 132:1139–46
57. Takahashi Y, Miyamoto T, Shiku H, Asano R, Yasukawa T, et al. 2009. Electrochemical detection of epidermal growth factor receptors on a single living cell surface by scanning electrochemical microscopy. *Anal. Chem.* 81:2785–90
58. Nagamine K, Onodera S, Kurihara A, Yasukawa T, Shiku H, et al. 2006. Electrochemical screening of recombinant protein solubility in *Escherichia coli* using scanning electrochemical microscopy. *Biotechnol. Bioeng.* 96:1008–13
59. Zhan D, Fan FRF, Bard AJ. 2008. The K_v channel blocker 4-aminopyridine enhances Ag^+ uptake: a scanning electrochemical microscopy study of single living cells. *Proc. Natl. Acad. Sci. USA* 105:12118–22
60. Goto M, Abe H, Ito-Saki T, Inagaki A, Ogawa N, et al. 2009. A novel predictive method for assessing the quality of isolated pancreatic islets using scanning electrochemical microscopy. *Transplant. Proc.* 41:311–13
61. Schrock DS, Baur JE. 2007. Chemical imaging with combined fast scan voltammetry–scanning electrochemical microscopy. *Anal. Chem.* 79:7053–61
62. Chen Z, Xie S, Shen L, Du Y, He S, et al. 2008. Investigations of the interactions between silver nanoparticles and HeLa cells by scanning electrochemical microscopy. *Analyst* 133:1221–28
63. Liebetrau MJ, Miller HM, Baur JE, Takacs SA, Anupunpisit V, Garriss PA. 2003. Scanning electrochemical microscopy of model neurons. *Anal. Chem.* 75:563–71
64. Ballesteros Katemann B, Schulte A, Calvo EJ, Koudelka-Hep M, Schuhmann W. 2002. Localised electrochemical impedance spectroscopy with high lateral resolution by means of alternating current scanning electrochemical microscopy. *Electrochem. Commun.* 4:134–38
65. Eckhard K, Schuhmann W. 2008. Alternating current techniques in scanning electrochemical microscopy (AC-SECM). *Analyst* 133:1486–97
66. Diakowski PM, Ding Z. 2007. Interrogation of living cells using alternating current scanning electrochemical microscopy. *Phys. Chem. Chem. Phys.* 9:5966–74
67. Bard AJ. 2008. Toward single enzyme molecule electrochemistry. *ACS Nano* 2:2437–40
68. Strein TG, Ewing AG. 1992. Characterization of submicron-sized carbon electrodes insulated with phenol-allylphenol copolymer. *Anal. Chem.* 64:1368–73
69. Wong DKY, Xu LYF. 1995. Voltammetric studies of carbon disk electrodes with submicrometer-sized structural diameters. *Anal. Chem.* 67:4086–90

70. Schulte A, Chow RH. 1998. Cylindrically etched carbon-fiber microelectrodes for low-noise amperometric recording of cellular secretion. *Anal. Chem.* 70:985–90
71. Slevin CJ, Gray NJ, Macpherson JV, Webb MA, Unwin PR. 1999. Fabrication and characterization of nanometre-sized platinum electrodes for voltammetric analysis and imaging. *Electrochem. Commun.* 1:282–88
72. Ballesteros Katemann B, Schuhmann W. 2002. Fabrication and characterization of needle-type Pt-disk nanoelectrodes. *Electroanalysis* 14:22–28
73. Chen S, Kucernak A. 2002. Fabrication of carbon microelectrodes with an effective radius of 1 nm. *Electrochem. Commun.* 4:80–85
74. Lee Y, Bard AJ. 2002. Fabrication and characterization of probes for combined scanning electrochemical/optical microscopy experiments. *Anal. Chem.* 74:3626–33
75. Watkins JJ, Chen J, White HS, Abruna HD, Maisonneuve E, Amatore C. 2003. Zeptomole voltammetric detection and electron transfer rate measurements using platinum electrodes of nanometer dimensions. *Anal. Chem.* 75:3962–71
76. Etienne M, Anderson EC, Evans SR, Schuhmann W, Fritsch I. 2006. Feedback-independent Pt nanoelectrodes for shear force-based constant-distance mode scanning electrochemical microscopy. *Anal. Chem.* 78:7317–24
77. Sun P, Mirkin MV. 2006. Kinetics of electron transfer reactions at nanoelectrodes. *Anal. Chem.* 78:6526–34
78. Takahashi Y, Hirano Y, Yasukawa T, Shiku H, Yamada H, Matsue T. 2006. Topographic, electrochemical, and optical images captured using standing approach mode scanning electrochemical/optical microscopy. *Langmuir* 22:10299–306
79. Zhang B, Galusha J, Shiozawa PG, Wang G, Bergren AJ, et al. 2007. Bench-top method for fabricating glass-sealed nanodisk electrodes, glass nanopore electrodes, and glass nanopore membranes of controlled size. *Anal. Chem.* 79:4778–87
80. Sun P, Mirkin MV. 2007. Scanning electrochemical microscopy with slightly recessed nanotips. *Anal. Chem.* 79:5809–16
81. Li Y, Bergmann D, Zhang B. 2009. Preparation and electrochemical response of 1–3 nm Pt disk electrodes. *Anal. Chem.* 81:5496–502
82. Amphlett JL, Denault G. 1998. Scanning electrochemical microscopy (SECM): an investigation of effects of tip geometry on amperometric tip response. *J. Phys. Chem.* 102:9946–51
83. Ludwig M, Kranz C, Schuhmann W, Gaub HE. 1995. Topography feedback mechanism for the scanning electrochemical microscope based on hydrodynamic forces between tip and sample. *Rev. Sci. Instrum.* 66:2857–60
84. Hengstenberg A, Kranz C, Schuhmann W. 2000. Facilitated tip-positioning and applications of non-electrode tips in scanning electrochemical microscopy using a shear force based constant-distance mode. *Chem. Eur. J.* 6:1547–54
85. Hengstenberg A, Blöchl A, Dietzel ID, Schuhmann W. 2001. Spatially resolved detection of neurotransmitter secretion from individual cells by means of scanning electrochemical microscopy. *Angew. Chem. Int. Ed.* 40:905–9
86. Pitta Bauermann L, Schuhmann W, Schulte A. 2004. An advanced biological scanning electrochemical microscope (BIO-SECM) for studying individual living cells. *Phys. Chem. Chem. Phys.* 6:4003–8
87. Ballesteros Katemann B, Schulte A, Schuhmann W. 2003. Constant-distance mode scanning electrochemical microscopy (SECM). Part I: Adaptation of a non-optical shear-force-based positioning mode for SECM tips. *Chem. Eur. J.* 9:2025–33
88. James PI, Garfias-Mesias LF, Moyer PJ, Smyrl WH. 1998. Scanning electrochemical microscopy with simultaneous independent topography. *J. Electrochem. Soc.* 145:L64–66
89. Lee Y, Ding Z, Bard AJ. 2002. Combined scanning electrochemical/optical microscopy with shear force and current feedback. *Anal. Chem.* 74:3634–43
90. Oyamatsu D, Hirano Y, Kanaya N, Mase Y, Nishizawa M, Matsue T. 2003. Imaging of enzyme activity by scanning electrochemical microscope equipped with feedback control for substrate-probe distance. *Bioelectrochemistry* 60:115–21

91. Yamada H, Fukumoto H, Yokoyama T, Koike T. 2005. Immobilized diaphorase surfaces observed by scanning electrochemical microscope with shear force based tip-substrate positioning. *Anal. Chem.* 77:1785–90
92. Wipf DO, Bard AJ, Tallman DE. 1993. Scanning electrochemical microscopy. 21. Constant-current imaging with an autoswitching controller. *Anal. Chem.* 65:1373–77
93. Kurulugama RT, Wipf DO, Takacs SA, Pongmayteegul S, Garriss PA, Baur JE. 2005. Scanning electrochemical microscopy of model neurons: constant distance imaging. *Anal. Chem.* 77:1111–17
94. Laforge FO, Velmurugan J, Wang Y, Mirkin MV. 2009. Nanoscale imaging of surface topography with the scanning electrochemical microscope. *Anal. Chem.* 81:3143–50
95. Alpuche-Aviles MA, Wipf DO. 2001. Impedance feedback control for scanning electrochemical microscopy. *Anal. Chem.* 73:4873–81
96. Ervin E, White HS, Baker LA. 2005. Alternating current impedance imaging of membrane pores using scanning electrochemical microscopy. *Anal. Chem.* 77:5564–69
97. Diakowski PM, Ding Z. 2007. Novel strategy for constant-distance imaging using alternating current scanning electrochemical microscopy. *Electrochem. Commun.* 9:2617–21
98. Macpherson JV, Unwin PR. 2000. Combined scanning electrochemical–atomic force microscopy. *Anal. Chem.* 72:276–85
99. Macpherson JV, Unwin PR. 2001. Non-contact electrochemical imaging with combined scanning electrochemical atomic force microscopy. *Anal. Chem.* 73:550–57
100. Kranz C, Friedbacher G, Mizaikoff B, Lugstein A, Smoliner J, Bertagnolli E. 2001. Integrating an ultramicroelectrode in an AFM cantilever: combined technology for enhanced information. *Anal. Chem.* 73:2491–500
101. Fasching RJ, Bai SJ, Fabian T, Prinz FB. 2006. Nanoscale electrochemical probes for single cell analysis. *Microelectron. Eng.* 83:1638–41
102. Maruyama K, Ohkawa H, Ogawa S, Ueda A, Niwa O, Suzuki K. 2006. Fabrication and characterization of a nanometer-sized optical fiber electrode based on selective chemical etching for scanning electrochemical/optical microscopy. *Anal. Chem.* 78:1904–12
103. Ueda A, Niwa O, Maruyama K, Shindo Y, Oka K, Suzuki K. 2007. Neurite imaging of living PC12 cells with scanning electrochemical/near-field optical and atomic force microscopy. *Angew. Chem. Int. Ed.* 46:8238–41
104. Isik S, Schuhmann W. 2006. Detection of nitric oxide release from single cells by using constant-distance-mode scanning electrochemical microscopy. *Angew. Chem. Int. Ed.* 44:7451–54
105. Böcker M, Fuchs H, Schäffer TE. 2009. Scanning ion conductance microscopy of cellular and artificial membranes. In *Nanotechnology*, Vol. 6: *Nanoprobes*, ed. H Fuchs, pp. 197–211. Weinheim: Wiley
106. Liu L, Wang Y, Zhang Y. 2009. Scanning ion conductance microscopy and its application in nanobiology and nanomedicine. *Adv. Mater. Res.* 60/61:27–30
107. Nitz H, Kamp J, Fuchs H. 1998. Combined scanning ion conductance and shear force microscopy. *Probe Microsc.* 1:1355185X
108. Böcker M, Anczykowski, Wegener J, Schäffer TE. 2007. Scanning ion conductance microscopy with distance-modulated shear force control. *Nanotechnology* 18:145505–10
109. Pastré D, Iwamoto H, Liu J, Szabo G, Shao Z. 2001. Characterization of AC mode scanning ion conductance microscopy. *Ultramicroscopy* 90:13–19
110. Mann SA, Hoffmann G, Hengstenberg A, Schuhmann W, Dietzel ID. 2002. Pulse-mode scanning ion conductance microscopy—a method to investigate cultured hippocampal cells. *J. Neurosci. Methods* 116:113–17
111. Nowak P, Li C, Shevchuk AI, Stepanyan R, Caldwell M, et al. 2009. Nanoscale live-cell imaging using hopping probe ion conductance microscopy. *Nat. Methods* 6:279–81
112. Happel P, Hoffmann G, Mann SA, Dietzel ID. 2003. Monitoring cell movement and volume changes with pulse-mode scanning ion conductance microscopy. *J. Microsc.* 212:144–51
113. Korchev YE, Gorelik J, Lab MJ, Sviderskaya EV, Johnston CL, et al. 2000. Cell volume measurements using scanning ion conductance microscopy. *Biophys. J.* 78:451–47
114. Gorelik J, Zhang Y, Shevchuk AI, Frolenkov GI, Sánchez D, et al. 2004. The use of scanning ion conductance microscopy to image A6 cells. *Mol. Cell. Endocrinol.* 217:101–8

115. Shevchuk AI, Gorelik J, Harding SE, Lab NJ, Klenermann D, Korchev YE. 2001. Simultaneous measurements of Ca^{2+} and cellular dynamics: combined scanning ion conductance and optical microscopy to study cardiac myocytes. *Biophys. J.* 81:1759–64
116. Shevchuk AI, Frolenkov GI, Sánchez D, James PS, Freedman N, et al. 2006. Imaging proteins in membranes of living cells with high-resolution scanning ion conductance microscopy. *Angew. Chem. Int. Ed.* 45:2212–16
117. Gorelik J, Ali NN, Shevchuk AI, Lab MJ, Williamson C, et al. 2006. Functional characterization of embryonic stem cell–derived cardiomyocytes using scanning ion conductance microscopy. *Tissue Eng.* 12:657–64
118. Mann SA, Meyer JW, Dietzel ID. 2006. Integration of a scanning ion conductance microscope into phase contrast optics and its application to the quantification of morphological parameters of selected cells. *J. Microsc.* 224:152–57
119. Shin W, Gillis KD. 2006. Measurement of changes in membrane surface morphology associated with exocytosis using scanning ion conductance microscopy. *Biophys. J.* 91:L63–65
120. Korchev YE, Negulyaev YA, Edwards CR, Vodyanoy I, Lab MJ. 2000. Functional localization of single active ion channels on the surface of a living cell. *Nat. Cell Biol.* 2:616–19
121. Pellegrino M, Orsini P, De Gregorio F. 2009. Use of scanning ion conductance microscopy to guide and redirect neuronal growth cones. *Neurosci. Res.* 64:290–96
122. Sánchez D, Anand U, Gorelik J, Benham CD, Bountra C, et al. 2007. Localized and noncontact stimulation of dorsal root ganglion sensory neurons using scanning ion conductance microscopy. *J. Neurosci. Methods* 159:26–34



Contents

An Editor's View of Analytical Chemistry (the Discipline) <i>Royce W. Murray</i>	1
Integrated Microreactors for Reaction Automation: New Approaches to Reaction Development <i>Jonathan P. McMullen and Klavs F. Jensen</i>	19
Ambient Ionization Mass Spectrometry <i>Min-Zong Huang, Cheng-Hui Yuan, Sy-Chyi Cheng, Yi-Tzu Cho, and Jentaie Shiea</i>	43
Evaluation of DNA/Ligand Interactions by Electrospray Ionization Mass Spectrometry <i>Jennifer S. Brodbelt</i>	67
Analysis of Water in Confined Geometries and at Interfaces <i>Michael D. Fayer and Nancy E. Levinger</i>	89
Single-Molecule DNA Analysis <i>J. William Efcavitch and John F. Thompson</i>	109
Capillary Liquid Chromatography at Ultrahigh Pressures <i>James W. Jorgenson</i>	129
In Situ Optical Studies of Solid-Oxide Fuel Cells <i>Michael B. Pomfret, Jeffrey C. Owrutsky, and Robert A. Walker</i>	151
Cavity-Enhanced Direct Frequency Comb Spectroscopy: Technology and Applications <i>Florian Adler, Michael J. Thorpe, Kevin C. Cossel, and Jun Ye</i>	175
Electrochemical Impedance Spectroscopy <i>Byoung-Yong Chang and Su-Moon Park</i>	207
Electrochemical Aspects of Electrospray and Laser Desorption/Ionization for Mass Spectrometry <i>Mélanie Abonnenc, Liang Qiao, BaoHong Liu, and Hubert H. Girault</i>	231

Adaptive Microsensor Systems <i>Ricardo Gutierrez-Osuna and Andreas Hierlemann</i>	255
Confocal Raman Microscopy of Optical-Trapped Particles in Liquids <i>Daniel P. Chorney and Joel M. Harris</i>	277
Scanning Electrochemical Microscopy in Neuroscience <i>Albert Schulte, Michaela Nebel, and Wolfgang Schubmann</i>	299
Single-Biomolecule Kinetics: The Art of Studying a Single Enzyme <i>Victor I. Claessen, Hans Engelkamp, Peter C.M. Christianen, Jan C. Maan, Roeland J.M. Nolte, Kerstin Blank, and Alan E. Rowan</i>	319
Chiral Separations <i>A.M. Stalcup</i>	341
Gas-Phase Chemistry of Multiply Charged Bioions in Analytical Mass Spectrometry <i>Teng-Yi Huang and Scott A. McLuckey</i>	365
Rotationally Induced Hydrodynamics: Fundamentals and Applications to High-Speed Bioassays <i>Gufeng Wang, Jeremy D. Driskell, April A. Hill, Eric J. Dufek, Robert J. Lipert, and Marc D. Porter</i>	387
Microsystems for the Capture of Low-Abundance Cells <i>Udara Dharmasiri, Makorzata A. Witek, Andre A. Adams, and Steven A. Soper</i>	409
Advances in Mass Spectrometry for Lipidomics <i>Stephen J. Blanksby and Todd W. Mitchell</i>	433
Indexes	
Cumulative Index of Contributing Authors, Volumes 1–3	467
Cumulative Index of Chapter Titles, Volumes 1–3	470

Errata

An online log of corrections to *Annual Review of Analytical Chemistry* articles may be found at <http://arjournals.annualreviews.org/errata/anchem>.